A NEW SIGNAL PROCESSING TECHNIQUE FOR ENHANCEMENT OF ULTRASONIC TESTING SIGNALS

F. Honarvar[1], S.A.M. Tabatabai[1], T. Dusatko and A.N. Sinclair [2]
[1,2] Department of Mechanical Engineering, K.N. Toosi University of Technology, Tehran, Iran
[3,4] Mechanical and Industrial Engineering, University of Toronto, Toronto, Canada

Abstract: One of the major problems with ultrasonic testing (UT) is the difficulty of interpretation of indications observed in UT signals. Examples of this situation are discrimination of closely-spaced reflectors as well as detection of discontinuities in coarse-grained materials, such as austenitic steel welds. A new signal processing technique for the improvement of time-resolution and signal-to-noise ratio of ultrasonic testing signals has been recently developed by the authors. This technique, which combines Wiener filtering and autoregressive spectral extrapolation in a new way, has shown to be quite effective in separating overlapping echoes and improving the signal-to-noise ratio of relatively noisy signals. It can reveal some details of UT signals which can not be observed in raw signals.
In this paper, we will review the principles of this new technique and will present experimental results in order to demonstrate its capabilities. The experiments include pulse-echo measurements of closely spaced reflectors and time-of-flight diffraction (TOFD) measurements of flawed specimens. Application of the proposed signal processing technique to A-scan and B-scan images results in considerable improvement of the time-resolution and signal-to-noise ratio.

Introduction: Ultrasonic testing (UT) can be a relatively difficult nondestructive testing technique for a novice to understand. One reason is the difficulty of interpretation of UT signals which are usually contaminated by noise and spurious signals. Lack of adequate time resolution is another problem which causes the UT echoes to overlap and in some cases makes the identification of individual echoes impossible. This problem is more serious in testing thin specimens.
There have been attempts to overcome these problems and to improve the time resolution and signal-to-noise ratio of UT signals. Various deconvolution techniques have been used for improving the time resolution. Hayward and Lewis [1] compared a number of different non-adaptive deconvolution techniques and concluded that Wiener filters are the best choice for on-line applications. Sin and Chen [2] studied various deconvolution techniques and found that the combination of Wiener filtering and autoregressive spectral extrapolation produces very good results. Miyashita *et al.* [3] used L1-norm deconvolution and spectral extrapolation for processing ultrasonic signals. In their study, signals with no noise or very high signal-to-noise ratio were considered. Zala *et al.* [4] used L1-norm and a combination of Wiener filtering and spectral extrapolation for analyzing ultrasonic signals. McRae [5] applied a number of deconvolution techniques, including Wiener filtering and spectral extrapolation, to signals obtained from adhesive joints in composites. In a recent paper Honarvar *et al.* [6] proposed a new technique for combining Wiener filtering and autoregressive spectral extrapolation which significantly improves the time resolution and signal-to-noise ratio of UT signals. In this paper, the principles of this new approach are reviewed and experimental results obtained from ultrasonic testing of various specimens are presented.
In mathematical terms, an ultrasonic signal, *y(t),* can be modeled as the convolution of the impulse response of the measurement system, *h(t),* with the impulse response of the flaw, *x(t),*

$$y(t) = h(t) * x(t) \quad (1)$$

where * denotes the linear convolution operator. Noise can be considered to be additive to this system and appears as an *n(t)* term in the equation,

$$y(t) = h(t) * x(t) + n(t) \quad (2)$$

In the frequency domain, the convolution term turns into simple multiplication. Therefore, in the frequency domain Eq. (2) is written as,

$$Y(\omega) = H(\omega)\ X(\omega) + N(\omega) \quad (3)$$

where $Y(\omega)$, $H(\omega)$, $X(\omega)$, and $N(\omega)$ are the Fourier transforms of *y(t), h(t), x(t),* and *n(t)*, respectively. In the frequency domain, the impulse response of the flaw, $X(\omega)$, can be obtained by a simple division. However, in most cases, this procedure is not stable and it happens that for certain values of *ω,* the denominator equals to zero. Using a least squares criterion, Wiener showed that a good estimate of $X(\omega)$ can be obtained from the following equation [3],

$$X(\omega) = \frac{Y(\omega)\ H^*(\omega)}{|H(\omega)|^2 + Q^2\ |H(\omega)|^2_{\max}} \quad (4)$$

where, $H^*(\omega)$ is the complex conjugate of the impulse response of the system, $H(\omega)$, and Q^2 is a frequency independent term called the noise desensitizing factor. Equation (4) represents a deconvolution technique called Wiener filtering.

One of the major challenges in applying deconvolution techniques, including Wiener filtering, is the selection of the reference signal *H(ω)*. For UT signals, the back-wall echo or an echo obtained from a known reflector can be used as the reference signal.

The resolution of the signals deconvolved by Wiener filtering can be further enhanced by another signal processing technique called autoregressive (AR) spectral extrapolation. In applying AR spectral extrapolation, it is assumed that the flaw impulse can be modeled as an autoregressive process. The frequency spectrum of the signal is calculated and a frequency band which has good signal-to-noise ratio is selected. The rest of the spectrum is then reconstructed by extrapolating this part of the spectrum. If performed appropriately, AR spectral extrapolation combined with deconvolution leads to a spectrum which is almost flat. The signal obtained after evaluating the inverse Fourier transform of the processed spectrum has much better time resolution and higher SNR compared to the original signal. However, in applying AR spectral extrapolation, a number of parameters must be arbitrarily assigned to the process. A new approach, which eliminates arbitrary selection of parameters and leads to a more robust process, was recently developed by the authors [6]. In this new approach, a relatively high order AR process is chosen and for the AR spectral extrapolation several frequency windows containing relatively high SNR are selected. Combining the results obtained from each window considerably reduces noise and yields better results.

Results: Experiments have been conducted on a variety of specimens using pulse-echo and time-of-flight diffraction (TOFD) ultrasonic testing techniques.

The first specimen was an aluminum block with a 1 mm side-drilled hole. The hole was located near the back-wall of the specimen, see Fig. 1.

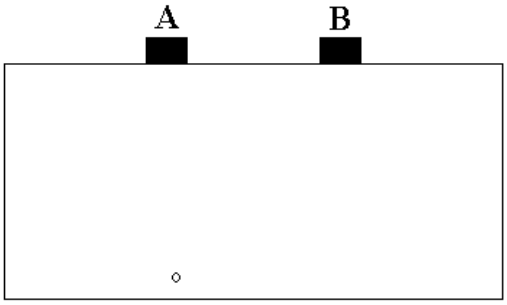

Fig 1: Aluminum block with side-drilled holes

A 12.7 mm (0.5") diameter, 1.0 MHz probe was used in this test. The reference signal was obtained from an unflawed section of the specimen. The raw and the processed signals corresponding to position A, featuring a single hole near the back-wall, are shown in Figure 1. It can be observed that although the existence of two reflectors, hole and the back-wall, cannot be easily distinguished in the raw signal, in the processed signal the two echoes are completely separated and the distance between the hole and the back-wall can be easily measured. Moreover, a third echo with opposite phase is observed shortly after the echo of the side-drilled hole. This echo is attributed to the interaction of the incident wave with the cylindrical hole. The reason for the existence of this echo is currently being investigated.

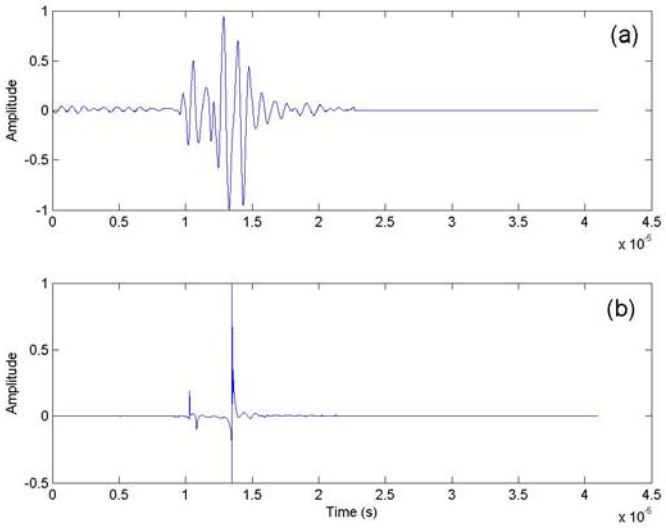

Fig 2: Signals obtained from the single side-drilled hole a) raw b) processed

Measurements were also conducted on steel blocks in which various artificial flaws were implanted. The ultrasonic time-of-flight diffraction (TOFD) technique was used in these measurements. In the TOFD technique, two angle beam probes with relatively high frequencies act in a pitch-catch mode. The transmitter probe sends angled longitudinal waves into the material. A typical arrangement for the TOFD test and the corresponding A-scan display are shown in Fig 3(a) and (b), respectively. When an internal crack lies between the two probes, three echoes appear before the back-wall echo on the A-scan display of the instrument. The four echoes on the A-scan display are named as shown in Fig 3(b) and each has its own phase as indicated by + and – sign. The echoes indicated by minus sign are 180 degrees out of phase with echoes indicated by plus sign.

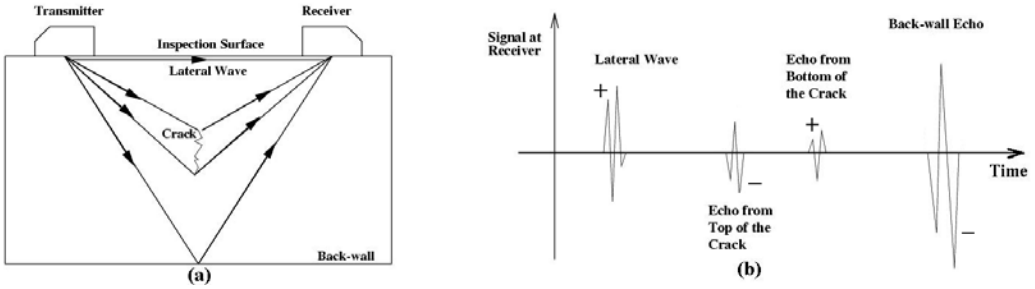

Fig 3: a) A typical TOFD arrangement, b) A-scan display of the TOFD test shown in (a)

In Fig. 3(a) the lateral wave travels beneath the top surface of the specimen and arrives earlier than other echoes. Two waves diffract from the top and bottom of the crack and arrive after the lateral wave. The back-wall reflection is the last echo observed on the display. In certain cases one or more of these four echoes might not appear on the display. For example, in the case of a crack open to the surface of the specimen, the lateral wave and the echo from the top of the crack do not appear on the display. On the other hand, if the crack is open to the back surface, only the lateral wave and the echo from the top of the crack can be seen on the display.

The TOFD experiments were conducted on 400 mm long steel blocks. The sides of the square cross section of the blocks were 38 mm each. Some of the blocks contained finely machined slots representing surface or internal cracks. These slots were created by an electro-discharge machining (EDM) process. Side-drilled holes were also machined in some of the blocks to represent other types of discontinuity. Three of these blocks containing surface and internal cracks and side-drilled holes are shown in Fig. 4.

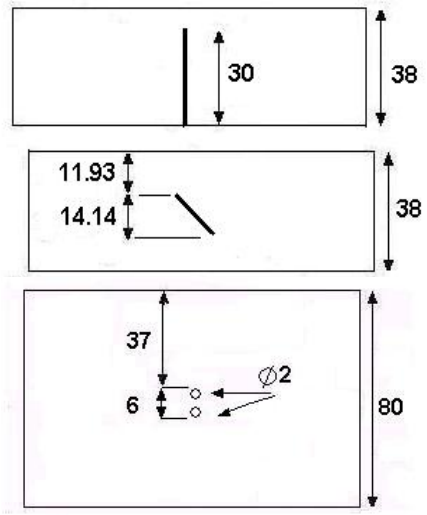

Fig 4: Steel blocks with implanted defects (all sizes are in millimeters)

The probes used for conducting the experiments were 3 mm in diameter and had a center frequency of 10 MHz. They generated longitudinal waves in the specimen at an angle of 60 degrees. The signals were collected by a Sonatest flaw detector and were digitized by a 100 MHz analog-to-digital converter before being sent to a computer for storage and further processing by the signal processing techniques described in this paper. A graphical user interface (GUI) was developed to facilitate the signal processing.

Discussion: The A-scan image of the raw data obtained from the steel block with a 30 mm deep back surface crack (see Fig. 4) is shown in Fig. 5. A back-wall echo measured from an unflawed part of the block was used as the reference signal in the deconvolution process.

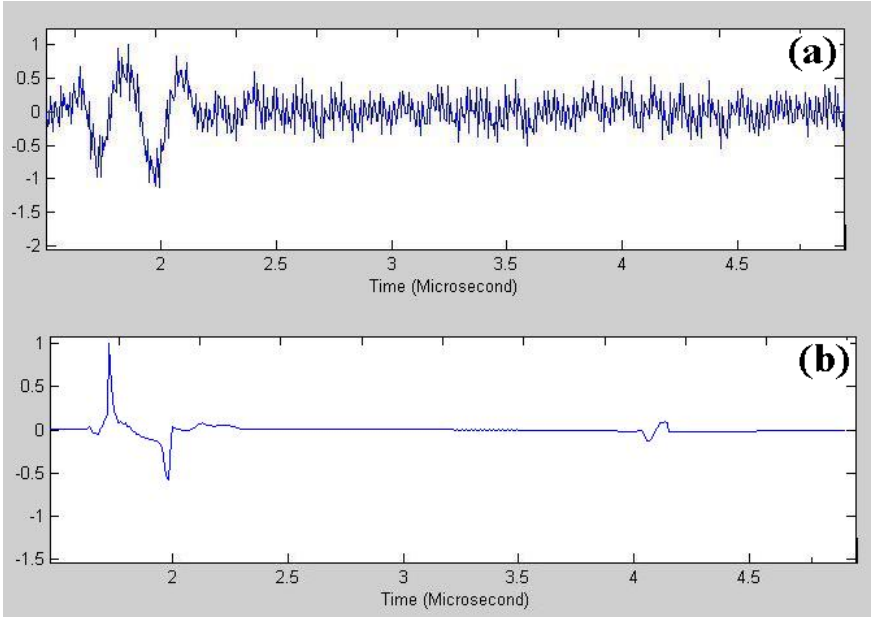

Fig 5: a) A-scan of the raw signal obtained from the steel block with 30 mm deep back surface crack, b) processed signal

It can be observed that in the raw signal, Fig 5 (a), the lateral wave and the echo originating from the top of the crack are merged together and cannot be resolved from each other. The signal-to-noise ratio (SNR) of the raw signal is also very low. In the processed signal, these two echoes are completely separated from each other and their relative phases can be clearly identified. The lateral wave was used as the reference signal in the deconvolution process.

The next experiment was performed on the steel block having an internal artificial crack shown in Fig. 4. In this experiment, it is expected that three distinct echoes would be observed before the back-wall echo, see Fig. 2(b). The raw and processed signals are shown in Figs 6 (a) and (b), respectively. Note that the back-wall echo is not shown in Fig 6. The lateral wave was taken as the reference signal in the deconvolution process. It can be observed that while the echoes are very weak in the raw signal, after the processing, the lateral wave and crack tip echoes and their corresponding phases can be easily distinguished. In TOFD measurements the depth of the crack can be estimated by measuring the difference between the arrival time of the lateral wave and first crack tip echo. The through-wall depth of the crack can also be calculated by measuring difference between the arrival times of the crack tip echoes. Clearly, these measurements can be done much more easily on the processed signal.

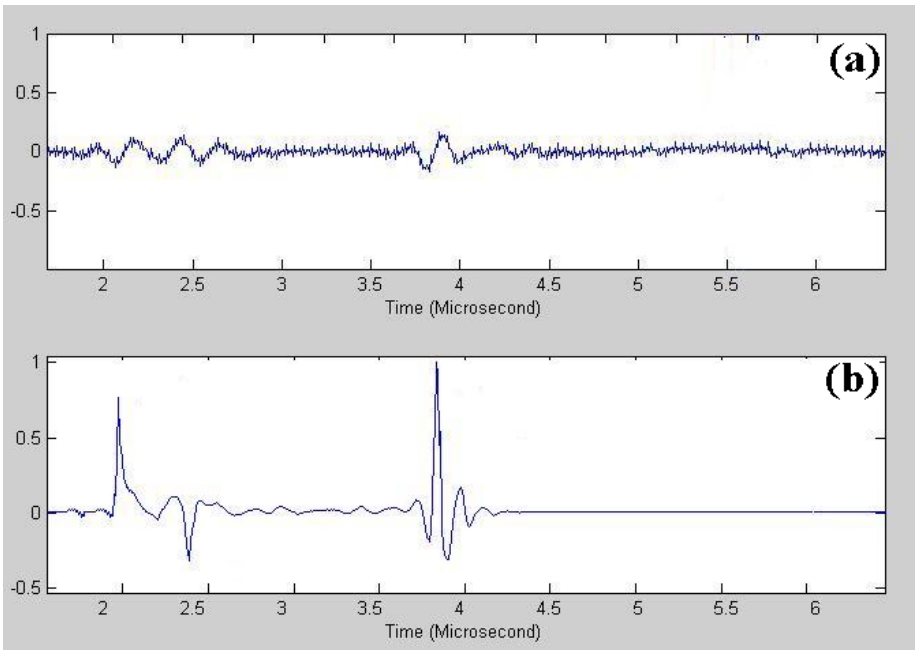

Fig 6: a) raw signal obtained from the internal crack b) processed signal. The back-wall echo is not shown

The third block contained two closely spaced 1 mm side drilled holes. The raw and processed signals for this specimen are shown in Fig. 7(a) and (b), respectively. In Fig. 7(a), the echoes coming from the two holes are completely overlapped and cannot be distinguished from each other. The processing of the signal has not only revealed the existence of two distinct targets, but has also unveiled the echoes diffracting from the top and bottom of each of the two holes. The size and depth of the two holes can be easily measured from the time difference of the diffracted echoes.

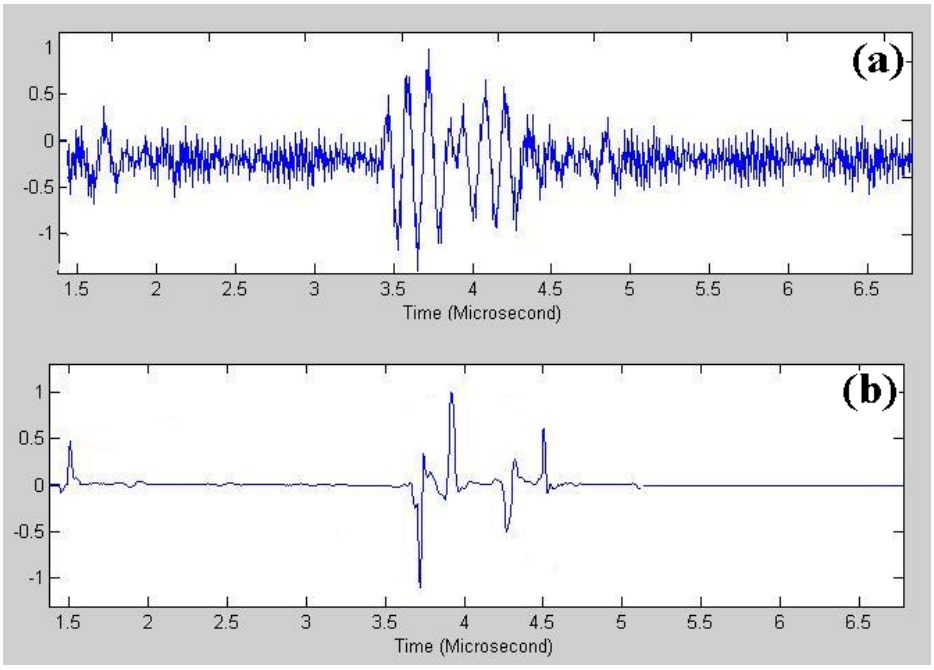

Fig. 7: a) raw signal obtained from the two holes drilled in the steel block b) processed signal

These results demonstrate the capability of the proposed signal processing technique in extracting valuable information that is buried in UT signals.
Measurements were also performed on real flaws. The specimens tested were 10 mm steel plate weldments. Various discontinuities such as crack, porosity, slag inclusion, etc. were implanted in the welds. The B-scan image obtained from one of these specimens which contained three flaws is shown in Fig 8. From left to right the three flaws are: 1) lack of side-wall fusion, 2) slag inclusion, and 3) root crack.

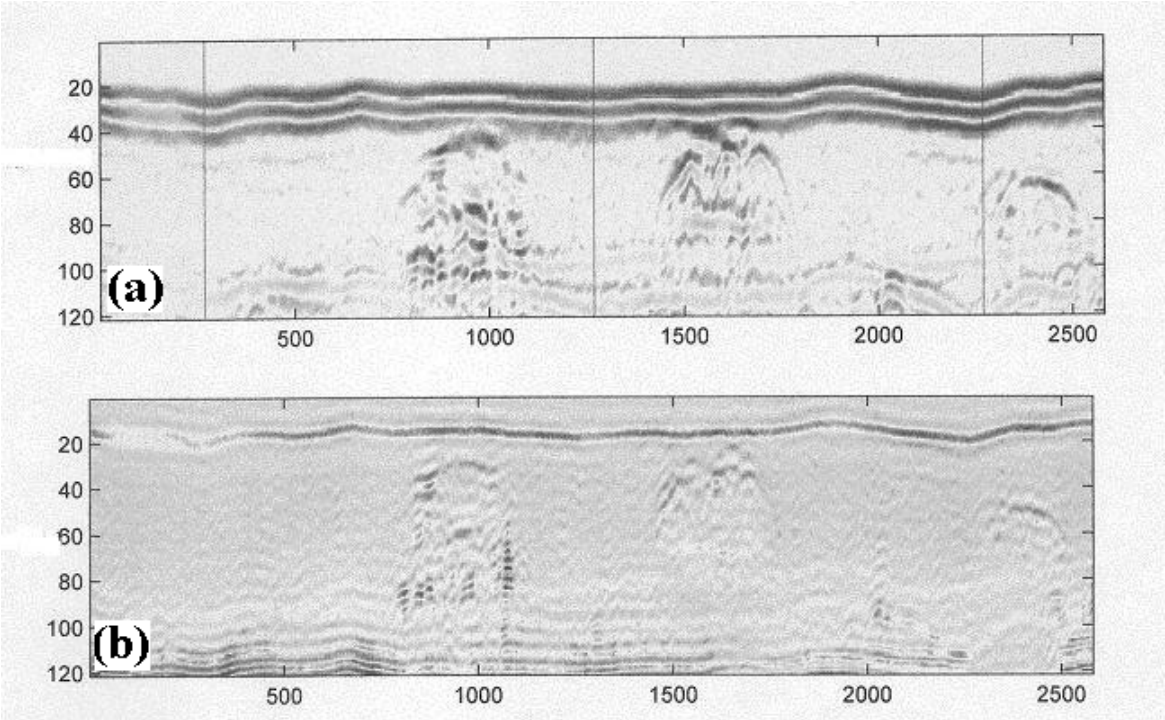

Fig 8: a) B-scan image of the weld b) processed B-scan image

The B-scan image of Fig. 8(a) consists of more than 2500 A-scan signals which are laid next to one another. Each A-scan signal was separately processed. The lateral wave was used as the reference signal. The dark horizontal line at the top of the image is the lateral wave.
Figure 8(b) shows that the processing of the B-scan image has considerably improved the SNR. The three implanted flaws can also be distinguished more easily in the processed image, although further work is required to optimize the technique.
Conclusions: Signal processing techniques can improve the quality of ultrasonic testing signals and help in the interpretation of results. A new approach that combines Wiener filtering and autoregressive spectral extrapolation was investigated in this paper. Experimental results from pulse-echo and time-of-flight diffraction measurements on ultrasonic A-scan and B-scan signals show considerable improvement in the time-resolution and signal-to-noise ratio. The processing of the UT signals reveals information which cannot be observed in the unprocessed signals. Work is currently underway to further enhance the robustness of the proposed process and make it suitable for on-line applications.

References:

[1] G. Hayward and J.E. Lewis. “Comparison of some non-adaptive deconvolution techniques for resolution enhancement of ultrasonic data.” *Ultrasonics*, 27:155-164, May 1989.

[2] Sam-Kit Sin and Chi-Hau Chen. “A comparison of deconvolution techniques for the ultrasonic nondestructive evaluation of materials.” *IEEE Transactions on Image Processing*, 1(1):3-10, January 1992.

[3] Toyokatsu Miyashita, Horst Schwelick, and Werner Kessel. “Recovery of ultrasonic impulse response by spectral extrapolation.” *Acoustical Imaging*, 14, 1985.

[4] C.A. Zala, I. Barrodale, and K.I. McRae. “High resolution deconvolution of ultrasonic traces.”
NATO {ASI} Series, Signal Processing and Pattern Recognition, 1:101-108, 1988.

[5] K.I. McRae. “Deconvolution techniques for ultrasonic imaging of adhesive joints.” *Materials Evaluation*, 1380-1384, November 1990.

[6] F. Honarvar, H. Sheikhzadeh, M. Moles and A.N. Sinclair, “Improving the Time-Resolution and Signal-to-Noise Ratio of Ultrasonic NDE Signals.” *Ultrasonics*, 41:755-763, 2004.